Indian Journal of Chemical Technology
Vol. 33, September 2026, pp. 671-686
DOI: 10.56042/ijct.v33i5.30504

Recent development in MOF-based thin film nanocomposite membranes for dye removal: A review

Vaibhav Singh Thakur, J. Anandkumar & Mahendra S. Gaikwad*

Department of Chemical Engineering, National Institute of Technology Raipur, Raipur -492010, Chhattisgarh, India

*E-mail: msgaikwad.che@nitrr.ac.in

Received 7 April 2026; accepted 23 July 2026

Sustainable and effective water treatment methods must be established, as the discharge of coloured effluents, particularly dyes from the textile and chemical industries, poses an alarming threat to the environment. This review focuses on recent developments in thin film nanocomposite (TFN) membranes based on metal-organic frameworks (MOFs) as nanofillers, aiming to address problems associated with conventional thin film composite (TFC) membranes. Methods for MOF synthesis and membrane fabrication, along with their characterizations, are discussed in this review. The performance of the various MOF-TFN membranes for different dye removal is systematically discussed. The integration of MOF significantly enhances the membrane's performance by enhancing water flux, improving dye rejection, and surface functionality. Ultimately, MOF-TFN membranes represent a pioneering process that paves the way for highly efficient, sustainable, and long-term water treatment solutions.

Keywords: Dye nanofiltration, Dye removal, Metal Organic Frameworks (MOF), Thin film composite membrane, Water treatment

Introduction

Water is essential to life, and its quality has a significant impact on ecosystems and human populations. The abundance of pollutants that have been discharged into streams and rivers in recent years due to expanding industry, the rise of urbanization, and agricultural operations, presents a potential risk for both the aquatic environment and individual well-being[1]. Almost 20% of the worldwide water contamination originates from pollution caused by textile industry operations, which makes it the second-leading polluter after the oil sector [2]. For each kilogram of item produced, the textile industry typically needs 200 L of drinkable water. Wet fabric processes and dry fabric processes are the two primary methods employed in the textile sector. A large percentage of liquid waste is created during the wet processing phase[3,4]. Contaminants found in wastewater include colouring agents, acids, bases, and solid inorganic and organic constituents like lignin and tannin. Different heavy metals, comprising mercury, arsenic, cobalt, copper, cadmium, nickel, lead, and compounds of sulfur and nitrates, are reported to be present in textile effluent, including carcinogenic organic materials like hydrocarbon-based softeners, non-biodegradable dyeing products, colour fixing agents based on formaldehyde, and stain removers containing chlorine [5].

In accordance with a recent study, over 70 lakh tons of dyes are synthesized each year[6–9]. Azo dyes make up over half of the dyes that are widely used globally, and due to ineffective textile dying techniques, around 15-50% of azo dyes that are not adhered to textiles and fibers end up in the wastewater effluent stream[10,11]. This incapability associated with the dye combination, the dye molecules and chemicals failing to fully bind to a fabric surface, is the root cause of the existence of dye-containing effluents in the textile sector. In general, materials intended for colouring are able to absorb nearly 80% of the dye pigment and chemical molecules from colouring solutions. Because of their limited adsorption capacity, textile materials can only absorb at most 20% of the dye[12].

These dyes possess a prolonged half-life in the surrounding environment if left untreated. For instance, the hydrolyzed Reactive Blue 19 has a half-life lasting roughly 46 years at pH level 7 and 25 °C [13]. By preventing light penetration, bleaching, lowering dissolved oxygen levels, and inhibiting photosynthetic activity, coloured effluents alter the stability of aquatic ecosystems. Human health risks

include allergic reactions to skin, burns within the eyes, and adverse effects on the liver, kidneys, and central nervous system when exposed to high concentrations of hazardous dyes and their breakdown products[6,11]. Electrochemical destruction, photochemical, Oxidation, including Advanced oxidation processes, ozonation, Fenton reaction, and UV irradiation are examples of classical chemical techniques for dye removal. However, in addition to being economically unappealing, chemical dye removal techniques also require specialized equipment and a significant amount of electrical energy. Another negative feature of this method that creates an additional disposal problem is the production of hazardous secondary pollutants after a chemical dye elimination process is completed[12]. One sustainable way to remove dye from textile wastewater with the least amount of expense and longest working duration is by biological approaches, such as bioremediation, which breaks down colours using biological phenomena, through biodegradation, bacteria, fungus, algae, plants, and yeasts all play important roles in the breakdown of dyes. Both aerobic and anaerobic microbial breakdown have positive outcomes. The biological reduction of dyes is facilitated by biodegradation techniques involving enzyme catalysis and biosorption[5,14]. They are associated with certain limitations like biomass accumulation, extended period of microbial buildup, difficulty in establishing ideal degrading conditions, ineffectiveness, enzyme's unstable nature, and decline in enzyme's activity[15]. Physical techniques for removing dye include coagulation or flocculation, adsorption, ion exchange, irradiation, and membrane filtration. These methods are usually straightforward procedures that are commonly performed utilizing the mass transfer mechanism[12,15]. Membrane-based separation techniques have several advantages over conventional separation methods like adsorption, absorption, and distillation, including low consumption of energy, low complexity, affordability, high selectivity, high scalability potential, and simple integration with other processes [16].

Nowadays, Polymeric membranes are an attractive option for wastewater treatment because of their direct pore-forming process, simplicity of installation, flexibility, and reasonable cost [17]. TFC membranes are often utilized in commercial RO and NF operations. Interfacial polymerization is the method used to directly fabricate the TFC selective layer above a porous substrate. The unique three-layer structure of the PA-TFC membrane is one of its characteristics. The primary component that can reject salts and serve as the primary transport resistance layer is the polyamide surface layer (PA) layer, which is created by IP and has a thickness of around 100 nm. Typically, polysulfone with a thickness of around 40 µm is used as a middle layer that provides support to the PA layer and the platform's IP. Additionally, mechanical strength is provided by the bottom non-woven supporting layer, with a thickness of approximately 120 µm [18].

The application of nanomaterials in membrane fabrication has demonstrated exceptional antifouling resistance. Selectivity, permeability, thermal stability, mechanical durability, surface charge, hydrophilic nature, and antimicrobial activity of polymeric membranes are influenced by the nanomaterials[17]. Several nanomaterials have been used to increase the performance of TFC membranes, including carbon quantum dots, nanotubes, metal oxides, graphene oxide, Mxene, zeolites, metal-organic frameworks (MOFs) and other nanomaterials[19–21].While silica and zeolite increase membrane performance relative to control membranes, adding nanomaterials in the active layer may reduce membrane selectivity. MOFs with organic linkers have a higher affinity for organic polymers compared to inorganic materials used as additives.In situ polymerization of the MOF-polymer composite results in the production of non-covalent bonds, such as hydrogen bonds, as well as covalent bonds, which contribute to the two phases' compatibility[19]. MOFs are a type of porous material that is both inorganic and organic. MOFs have advantages over other porous nanomaterials, such as low skeleton density, high specific surface area, configurable pore structures, and functional modifications. MOFs are ideal for membrane science, adsorption, gas storage, catalysis, and chemical sensing due to their high specific surface area, high crystallinity, and great thermal and chemical durability[21,20]. MOF-based MMMs, which use MOFs as fillers inside the continuous polymer matrix, have shown potential as membrane fillers to overcome the disadvantages associated with pure polymers[22]. MOFs are a novel kind of composite material that assembles itself using organic linkers and metal ions or clusters. With its high porosity, adjustable pore size, and large surface area, MOF performs better than conventional materials such as zeolite and clay[23]. The efficiency of

membrane separation is significantly improved by using a polymer matrix, which provides superior processability and mechanical durability, coupled with nanoporous MOF fillers with an adjustable pore structure for efficient gas transport and molecular sieving [22]. The objective of this comprehensive review is to explore the latest developments in MOF-TFN membranes, with a focus on synthesis processes and the assessment of their separation capabilities for dye removal.

MOF synthesis

The Cambridge Structural Database (CSD) contains roughly 95,000 distinct MOF structures, indicating the rapidly developing field of research. However, the scalability of MOF synthesis processes is challenging, but current research is addressing this limitation by the introduction of novel synthesis methods such as microwave-assisted, mechanochemical, and green solvent synthesis[24]. The reaction temperature plays an important role in the MOF synthesis. There are also two temperature ranges: solvothermal and non-solvothermal, which are widely recognized and used to describe the types of reaction setups that must be employed. Solvothermal reactions take place within closed containers under autogenous pressure beyond the solvent's boiling point. A non-solvothermal reaction occurs at or below the boiling point under ambient pressure[25]. MOFs are typically produced through solvothermal or hydrothermal processes operating at high temperatures and pressures. This method is a 'classic' approach for MOFs synthesis. Other approaches, including mechanochemical, electrochemical, microwave, sonochemical, and electrochemical, have emerged in recent years. They are cost-efficient as well as rapid, with superior results [26]. The following section includes different methods utilized in MOF synthesis.

Solvothermal synthesis

In Solvothermal synthesis, crystals form under elevated pressure and temperature. Traditional solvothermal synthesis is carried out by heating the organic linker and metal ions in a solvent, inside a glass bottle for low temperature ranges or in a Teflon-coated autoclave, or bomb reactor for temperatures beyond ~ 400 K, moment the boiling point of the solvent is reached, it may dissolve completely or partially. Crystals are formed as a result of precipitation. They may require several hours or even days to finish, and the reactions happen in autoclaves using polar solvents at temperatures ranging from 50°C to 260°C. Temperature, Pressure, solvent composition, and other parameters are all adjusted in order to achieve a certain structure [26–28]. Fig. 1a illustrates the schematic for the solvothermal synthesis of MOF.

Hydrothermal synthesis

The hydrothermal synthesis process uses high temperatures and pressures to assist the dissolution of substances that are insoluble under standard environmental conditions. Such a process is typically carried out in an autoclave using water-based solvents. This approach involves dissolving precursors in heated water under elevated pressure. The prepared solution mixture is transferred to the pressure vessel (autoclave) and further heated to elevated temperatures. After the completion of reaction, the autoclave was allowed to return to ambient conditions. The supernatant was separated, rinsed repeatedly with deionized water and alcohol, and then dried to obtain the end product[29].

Microwave-assisted synthesis

Microwaves are a form of non-ionizing electromagnetic waves with frequencies ranging from 300 MHz to 30 GHz. When microwaves penetrate materials, the microwave's radiation energy is converted into heat, primarily through ionic conduction for charged species and dipolar polarization for molecules with dipoles [30].

These characteristics make it a suitable candidate for future uses.[31] Cr-MIL-100, reportedly the first MOF was synthesized using Microwave heating at 220°C for 4 h. The process was further improved by lowering the time to 1 h, providing the MOF with equivalent textural and physicochemical characteristics [32]. The microwave-assisted approach allows for the synthesis of different MOFs, which can be further classified into MW-assisted solvent synthesis, MW-assisted solvent-free synthesis, MW-assisted ball milling synthesis, and MW-assisted continuous-flow synthesis [33]. Fig. 1b illustrates the schematic for the microwave-assisted synthesis of MOF.

Sonochemical synthesis

Sonochemical synthesis yields smaller particles in a shorter period than standard solvothermal synthesis. A reaction solution mixture for MOF construction is

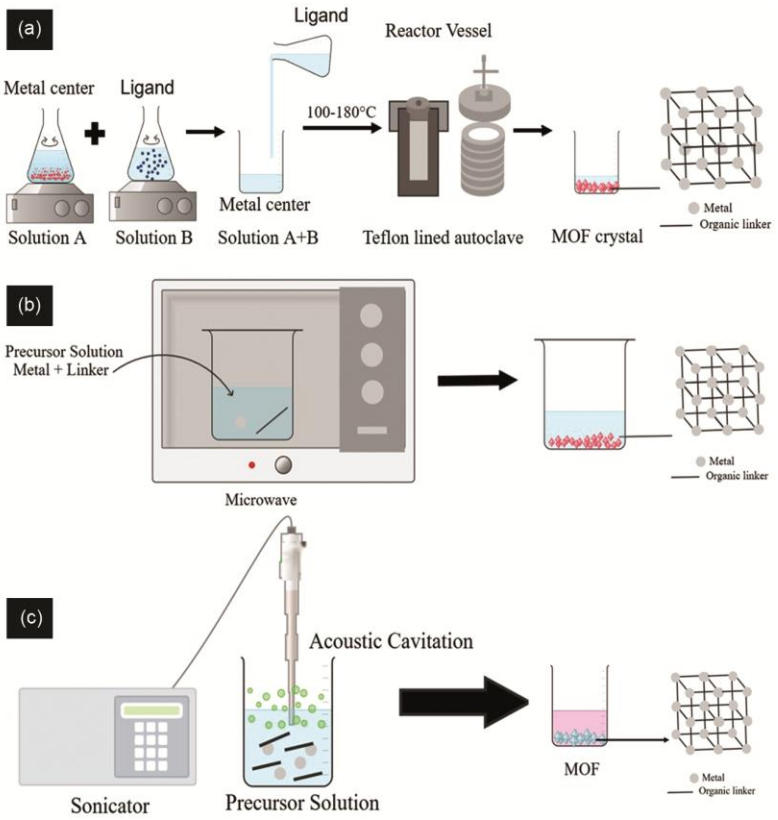

Fig. 1 — (a) Conventional solvothermal synthesis, (b) microwave-assisted synthesis and (c) sonochemical synthesis

placed into a pyrex vessel equipped with a sonicator probe that has configurable power output. Acoustic cavitation, the creation and collapse of bubbles in a solution after sonication, generates extremely high localized temperatures (~5,000 K) and pressures (~1,000 bar). This leads to rapid cooling and heating rates (>1010 K/s) and formation of fine crystals.[34]. Fig. 1c illustrates the schematic for the sonochemical synthesis of MOF.

Slow evaporation synthesis or room temperature synthesis

This approach eliminates the need for an external energy source because the reaction takes place at room temperature. Mixed reagents are used in a slow evaporation process, which allows them to evaporate gradually. Crystals start to form when a critical concentration is reached, which encourages crystal nucleation and growth. To accelerate the procedure, a combination of low-boiling-points solvents is commonly used [26,28]. Fig. 2a shows the schematic for this synthesis method.

Mechanochemical synthesis

A blend of metallic salt and organic ligand is crushed in a mortar, pestle, or ball mill without employing any solvent. After milling, the blend is gently heated to remove moisture or other volatile compounds generated as secondary products of the reaction mixture. This approach involves breaking intermolecular bonds with mechanical force, followed by a chemical reaction[35]. Fig. 2b illustrates the schematic for this synthesis method. This method of synthesis is solvent-free, or sometimes uses minimal solvents and is a solid-state organic approach that eliminates harmful solvents. The solid-solid interaction allows for large-scale material manufacturing and easy handling, as it yields powdered products[36]. When a small amount of solvent is introduced, the resulting process can be termed as liquid-assisted grinding (LAG) [35].

Electrochemical synthesis

The electrochemical approach of MOFs employs electrons as a supplier of metallic ions, which are transmitted through a reaction solution, which contains dissolved organic ligands and an electrolyte by anodic dissolution serving as the metal source rather than conventional metal salts[35]. Fig. 2c illustrates the schematic for this synthesis route. In 2005, the first MOF produced using an electrochemical technique was HKUST-1, also known as Cu-MOF. BASF

researchers were the first to report on MOF synthesis via an electrochemical route. They established new synthesis processes for certain MOFs employing Cu, Zn, Co, and Mg as cathode materials and 1,3,5-H_3BTC and 1,2,3-H_3BTC, H_2BDC, and H_2BDC-$(OH)_2$ as linkers. The electrochemical MOF synthesis technique is classified into three categories based on the direction of electron transfer and the location of nucleation sites: electrode-surface nucleation (ESN), indirect bipolar electrodeposition (IBED), and electrophoretic deposition (EPD). The first two techniques rely on the instantaneous generation of MOFs in the reaction system, whereas EPD is based on MOF pre-synthesis and deposition[37].

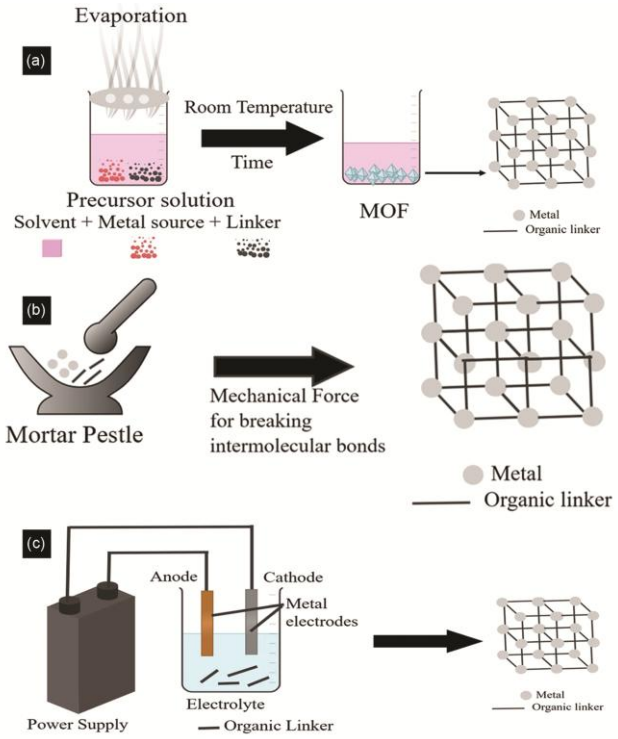

Fig. 2 — (a) Slow evaporation synthesis (b) mechanochemical synthesis and (c) electrochemical synthesis

Layer-by-layer synthesis

Surface-Mounted Metal Organic Frameworks (SURMOFs) are produced by layer-by-layer at room or low temperature, with the reactants kept apart rather than combined, and film growth is accomplished by repeated, sequential immersion in two solutions of the organic linker and metal source. To create SURMOFs, the substrate must be functionalized so that a certain functional group, such as a COOH, OH, or pyridyl group, is exposed. SURMOF preparation usually consists of three steps: 1) Substrate selection, 2) surface functionalization to promote anchoring MOF building units, and 3) layer-by-layer deposition of SURMOFs via subsequent immersion[38]. HKUST-1 [$Cu_3(BTC)_2.n(H_2O)$] MOF was the first successful type of MOF studied and synthesized utilizing the LBL method[39]. Fig. 3 illustrates a schematic for the layer-by-layer synthesis.

Microfluidic synthesis

Microfluidics is a chemical synthesis technology that uses chips to regulate fluid flows at the micro-and nanoscales. This approach allows for the continuous manufacturing of MOFs by controlling precise parameters in synthesis, indicating a step toward intensification, adaptability, and scalability in the usage of MOFs[40],[41] engineered an interfacial microfluidic membrane processing (IMMP) approach for growing continuous ZIF-8 membranes on the inner surfaces of poly(amide-imide) (Torlon) hollow fibers. [42] reported microfluidic synthesis of ZIF-8 and ZIF-93 on a polysulfone hollow fibre support using methanol as solvent and Sodium formate as a modulator at room temperature. Table 1 summarizes the synthesis methods and conditions of different MOFs used as nanofillers in TFN membranes for dye removal.

TFC Membrane synthesis and MOF incorporation

Different fabrication methods such as IP, polymer melt blending and solution mixing are utilized in TFC

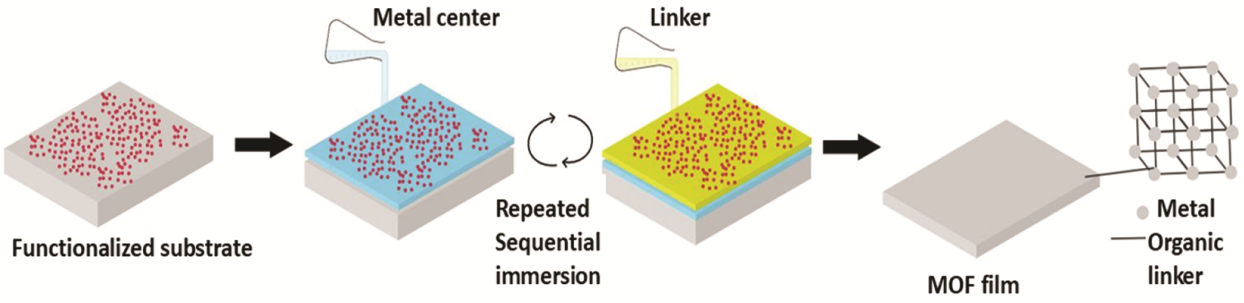

Fig. 3 — Layer-by-layer synthesis

membrane casting, among which IP has proven to be the most prominent ever since its introduction in 2007[57]. MPD and TMC are the two monomers most frequently utilized in TFC membrane fabrication are dissolved in different aqueous and organic solutions respectively. The polymerization reaction occurs at the water-organic solvent interface, resulting in a thin PA layer on the substrate by the IP method[58]. The schematic of IP process can be observed in Fig. 4. MPD interacts with TMC, starting nucleophilic

Table 1 — Synthesis methods and conditions of different MOFs used as a nanofiller in TFN membrane for dye removal

S. No.	MOF	Metal centre	Metal source / precursor	linker	Synthesis method	Synthesis solvent	Modulator	Synthesis condition		Ref.
								Temperature	Time	
1.	UiO-66	Zr^{4+}	$ZrCl_4$	BDC (1,4-benzenedicarboxylate)	Solvothermal	Water	Acetic acid	Room temperature	2 h	43
				BDC (1,4-benzenedicarboxylate)	Solvothermal	DMF	Water	120°C	24 h	44
2.	MOF-808	Zr^{4+}	$ZrCl_4$	BTC (benzene -1,3,5-tricarboxylate)	Solvothermal	Water	Acetic acid	Room temperature	2 h	43
3.	ZIF-8	Zn^{2+}	Zn $(NO_3)_2.6H_2O$	2-methylimidazole	in situ synthesis					45
					Slow evaporation	Methanol	Water	Room temperature	2 h	44
					Room temperature synthesis, Microfluidic synthesis	Methanol	-	Room temperature	30 min	42,46
			$Zn(CH_3COO)_2.2H_2O$	2-methylimidazole	Interfacial synthesis	-	-	Room temperature	-	47
4.	MIL-101 (Cr)	Cr^{3+}	$CrCl_3.6H_2O$	BDC (1,4-benzenedicarboxylate)	Microwave-assisted	Water	-	180°C	30 min	42,48
			$CrCl_6.H_2O$	BDC (1,4-benzenedicarboxylate)	Microwave-assisted	Water	-	179.85°C	30 min	49
5.	ZIF-93	Zn^{2+}	Zn $(NO_3)_2.6H_2O$	4-methyl-5-imidazolecarboxaldehyde	Microfluidic synthesis	Methanol	Sodium formate	-	-	42
					Layer-by-layer	Methanol	-	-	-	50
						Methanol	Sodium formate	-	-	51
					Room temperature synthesis	Methanol	-	Room temperature	20 min	44
6.	Fe MOF	Fe^{3+}	$FeCl_3.6H_2O$	Fumaric acid	Hydrothermal	Water	-	65°C	12 h	52
7.	Ag MOF	Ag^{2+}	$AgNO_3$	BDC (1,4-benzenedicarboxylate)	Solvothermal	DMF	-	140°C	10 h	53
8.	Zr porphyrin MOF	Zr^{4+}	$ZrCl_4$	Ni-TCPP, Nickel-tetrakis(4-carboxyphenyl)-porphyrin	Solvothermal	DMF	Acetic acid, water	120°C	24 h	54
9.	HKUST-1	Cu^{2+}	$Cu(NO_3)_2.3H_2O$	BTC (benzene -1,3,5-tricarboxylate)	Hydrothermal	Water	Ethanol	110°C	18 h	55
			$Cu(OAc)_2$	H_3-BTC (benzene -1,3,5-tricarboxylate)	in-situ synthesis	Water	Ethanol	Room temperature	-	56

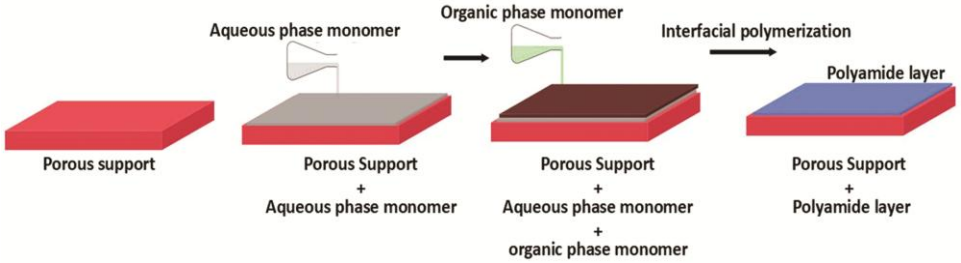

Fig. 4 — Interfacial polymerization for polyamide active layer synthesis

substitution, in which an amine group attacks TMC's carbonyl carbon, forming an amide bond and releasing hydrochloric acid (HCl). This process continues as successive MPD monomers react with TMC, forming a cross-linked PA structure and releasing byproducts like HCl and water. The final output is a strong, highly cross-linked PA network that constitutes the membrane's active selective layer.[59]. This method produces membranes with improved characteristics, such as increased performance, exceptionally high permeance, excellent rejection rates, and uniform polymerization, in addition to thermal and chemical stability [60]. Mogan was the first to suggest creating a thin polymeric layer on a substrate via interfacial polycondensation in order create a composite membrane. Cadotte and colleagues optimized formation condition to create composite membranes exhibiting elevated flux by crosslinking piperazine with a mixture of isophthaloyl chloride and trimesoyl chloride [61].

The most commercially successful membrane is the TFC polyamide membrane, which is created utilizing interfacial polymerization of two monomers MPD and TMC on a porous support. Polysulfone and polyethersulfone (PES) membranes created via the phase inversion process are frequently used as conventional TFC porous support membrane materials due to their superior temperature resistance, chemical robustness, and ease of production. Polyacrylonitrile (PAN), poly (ether sulfone) (PSF), polyvinylidene fluoride (PVDF), poly (arylene ether nitrile ketone) (PPENK), polyimide (PI), polytetrafluoroethylene (PTFE), and polypropylene (PP) are common polymeric support materials. Fig. 5 illustrates the schematics for support layer fabrication. The majority of effective TFC RO membranes have a notably hydrophobic support, leading to a PA thin with a significant salt rejection.[62]. The PA active layer separates pollutants throughout the filtration process, whereas the middle micro-porous layer protects the ultra-thin active layer against intense pressure during NF or RO operations. The TFC membrane's performance is evaluated by analyzing and comparing the characteristics of the effluent and influent. Recent research focuses on improving the physical and chemical characteristics of TFC membrane layers to enhance water flux and salt/contaminant removal. This includes pore size, hydrophilicity, strength, thickness, and roughness [58].

Numerous factors, including monomer concentrations, curing time, and curing temperature, might affect the process of desalination and morphological characteristics of the PA selective layer. [63] studied how a TFC membrane's morphology changed when the monomer concentrations of TMC and MPD were changed. The authors came to the conclusion that the extent of cross-linking was connected with the ratio of MPD/TMC concentrations, and that raising the ratio would result in a rise in salt rejection. Additionally, the researchers came to the conclusion that less cross-linking resulted from unreacted acyl chloride functionalities are produced by a lower MPD/TMC ratio[64]. The monomer concentration ratio has a considerable effect on the cross-linking density and thickness of the PA selective layer. Higher MPD concentrations create dense cross-linked structures that improve salt rejection but decrease water permeability, whereas lower concentrations produce thinner, more hydrophilic films. Increasing the TMC concentration, on the other hand, improves the hydrophilicity and cross-linking of the PA selective layer while also reducing flow due to increased thickness[59].

The most effective desalination membranes on the market right now are believed to be TFC membranes. Compared to conventional asymmetric membranes, these membranes increase productivity and selectivity while using less energy. In 1963, Loeb and Sourirajan fabricated a cellulose acetate membrane with a sodium chloride (NaCl) rejection of 98%.[65]. The

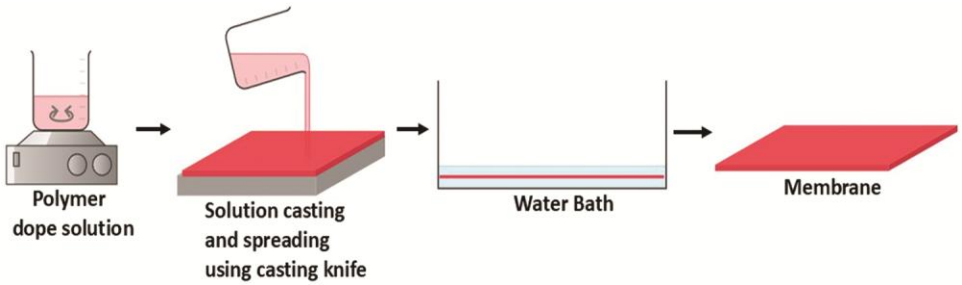

Fig. 5 — Support layer synthesis by non vapour induced phase inversion

ability to control and tune each layer separately to enhance its functionality is one of a TFC's significant features. It is possible to achieve a high solvent flux without sacrificing salt rejection [57]

Due to their high fouling tendency, low chemical stability, and poor chlorine tolerance, TFC membranes based on polyamide experience difficulties in real-world practices. Water permeability and membrane selectivity are compromised due to their extremely cross-linked and amorphous structure's lack of porosity and interconnectivity. Low water permeability is frequently implied by high salt rejection [64]. Recent research tries eliminate these challenges using advanced modifications and material advancements. Some current techniques for PA TFC include surface functionalization, nanoparticle inclusion, and hybrid polyamide. Surface changes increase hydrophilicity, reducing fouling by minimizing contaminant attachment to the membrane surface. Incorporating nanomaterials, like metal-organic frameworks (MOFs), silver nanoparticles, and graphene oxide has improved membrane stability, permeability, and selectivity. Furthermore, improvements in the IP technique for creating the selective PA layer have enabled researchers to tune monomer compositions, reaction conditions, and substrate materials. These improvements resulted in more homogeneous and defect-free PA layers, which improved membrane performance under different operational situations. [59].

The traditional method for producing MMMs involves growing MOF crystals in situ inside a combination that includes a MOF precursor solution including organic linkers and metal ions, along with a polymer suspension. This polymer present during MOF crystallization provides homogenous distribution of the filler throughout the matrix and enhances interfacial compatibility through steric hindrance and chain entanglement [66]. The MOF-modified have been fabricated through two principal strategies: the blending interfacial polymerization route and the preloading interfacial polymerization route. In the blending technique, MOF nanoparticles are first dispersed with TMC in n-hexane and then incorporated into the selective layer, while in the preloading technique, the nanoparticles are deposited upon the polysulfone substrate prior to the IP reaction [67].

Even though MOFs remain appealing within aqueous-phase modifiers for improving PA selective layer's efficiency, however aqueous PIP or MPD solution's alkalinity restricts usage for many superior-performing MOFs. In contrast, when incorporated through aqueous-phase, TFN membranes tend to show increased surface irregularity but only modest improvement in water flux. Their surface typically reflects the granular form of the embedded MOF, leading to surface characteristics that largely mirror those of the incorporated MOF [68,43,69,70], reported MOF TFN membrane by dispersing the MOF in aqueous phase while [44,70,42,49] reported membrane TFN synthesis by dispersion in organic phase. Table 2 presents a systematic tabulation for different membrane fabrication used in dye removal covering different reaction conditions.

Characterization of MOF and MOF-TFN membranes

Different characterization techniques used in analysis of the MOF and the TFN membrane are presented in Table 3. These techniques include TEM, SEM, STEM, and AFM to study the morphological characteristics and physical structures; XRD for crystalline structure; EDS, EDX, XPS, and ICP for elemental and compositional analysis; TGA to study thermal stability; FTIR for the chemical bonding and functional group analysis; BET, MWCO and pore size for porosity; Zeta potential and Water contact angle for surface properties.

Mechanism of dye separation in MOF-TFN membrane and performance analysis

The selection of a membrane process and its corresponding rejection mechanism is primarily determined by the driving force and the characteristics of the solute to be separated. For example, pressure-driven procedures like microfiltration (MF) and ultrafiltration (UF) rely on size exclusion. MF is commonly used to remove macro-sized molecules (>0.1 μm), such as bacteria and suspended solids, while UF is suitable for smaller molecules (0.01-0.1 μm), such as proteins and viruses. Nanofiltration (NF) combines size exclusion with Donnan exclusion, making it suitable for even smaller solutes (1-10 nm), including multivalent ions, dyes and fertilizers. Reverse osmosis (RO) employs a solution-diffusion mechanism making it ideal for rejection of nearly all solutes, including monovalent ions (<1 nm)[60]. NF membranes separate through size exclusion and electrostatic repulsion, commonly referred to as the Donnan effect. The size exclusion effect screens dye molecules based on membrane pore size,

Table 2 — Fabrication conditions and reaction parameters for MOF-TFN membrane used in dye removal

S. No.	MOF	Incorporation method	MOF loading (wt.%)	Porous support polymer	Aqueous phase monomer	Wt.%	Reaction time	Organic phase monomer / solvent	Wt.%	Reaction time	MOF position	Ref.
1.	UiO-66	Dispersion (aqueous phase)	0.01	Polyimide - PI (P84)	MPD	2	2 min	TMC/n-hexane	0.1	2 min	PA layer and Interlayer	43
		Dispersion (organic phase)	0.2	Polyimide - PI (P84)	MPD	2	2 min	TMC/ n-hexane	0.1	1 min	PA layer	44
2.	UiO-66-NH_2	Direct dispersion (aqueous phase)	0.01	Polyimide - PI (P84)	MPD	2	2 min	TMC/ n-hexane	0.1	2 min	PA layer and Interlayer	43
3.	Ag-UiO-66-NH_2	Dispersion (aqueous phase)	0.4, 0.6, 0.8	Polyethersulfone - PES	PPD	-	2 min	m-benzoyl chloride/ n-hexane	-	2 min	PA layer	69
4.	UiO-66-$(NH_2)_2$	Dual polymerization (organic phase)	0.004,0.006,0.008,0.02,0.04,0.06,0.08 and 0.1	Polysulfone - PSF	PIP	1	3 min	TMC/ n-hexane	0.15	1 min	PA layer	70
5.	MOF-808	Dispersion (aqueous phase)	0.01	Polyimide - PI (P84)	MPD	2	2 min	TMC/ n-hexane	0.1	2 min	PA layer and Interlayer	43
6.	ZIF-8	Position induced nanoporous surface (PINS)	-	Polypropylene -PP (amino functionalized via DIAP)	MPD with SDS	2 (MPD) and 0.1 (SDS)	2 min	TMC/ n-hexane	0.15	60 sec	Support layer	45
		Dispersion (organic phase)	0.2	Polyimide - PI (P84)	MPD	2	2 min	TMC/ n-hexane	0.1	1 min	PA layer	44
		Dispersion (organic phase) and Microfluidic in-situ crystallization	0.025	Polysulfone Hollow fiber -PSF HF	MPD	2	10 min	TMC / n-hexane	0.01	1-9 min	PA layer and Interlayer	42
		In-situ Interfacial synthesis	-	Polyacrylonitrile- PAN	PIP	2	10 min	TMC/ chloroform	0.1		PA layer	47
7.	MIL-101 (Cr)	Dispersion (organic phase)	0.025, 0.05	Polysulfone Hollow fiber -PSF HF	MPD	2	10 min	TMC / n-hexane	0.01	1-9 min	PA layer	42
		Dispersion (organic phase)	0.2	Langmuir−Blodgett (LB) modified Polyimide - PI (P84)	MPD	2	2 min	TMC / n-hexane	0.1	1 min	PA layer	49

(*Contd*.)

Table 2 — Fabrication conditions and reaction parameters for MOF-TFN membrane used in dye removal (*Contd*.)

S. No.	MOF	Incorporation method	MOF loading (wt.%)	Porous support polymer	Aqueous phase monomer	Wt.%	Reaction time	Organic phase monomer / solvent	Wt.%	Reaction time	MOF position	Ref.
8.	ZIF-93	Direct crystallization on support followed by IP	-	Polysulfone Hollow fiber -PSF HF	MPD	2	10 min	TMC / n-hexane	0.01	1-9 min	Interlayer	42
		In-situ liquid-phase deposition		Polyimide - PI (P84)	MPD	2	2 min	TMC / n-hexane	0.1	5 min	Intermediate layer between SWCNT and PA layer	50
		Microfluidic in-situ crystallization		Polyimide Hollow fiber -PI (P84) HF	MPD	2	5 min	TMC / n-hexane	0.3	1.5 min	Interlayer	51
		Dispersion (organic phase)	0.2	Polyimide - PI (P84)	MPD	2	2 min	TMC/ n-hexane	0.1	1 min	PA layer	44
9.	Ag MOF	Dispersion (aqueous phase) vacuum filtration	0, 0.005, 0.01, 0.015 and 0.02	Poly (vinylidene fluoride) - PVDF	PIP with NaOH and triethylamine (TEA)	2 (PIP), 0.2 (NaOH) and 0.5 (TEA)	3 min	TMC / n-hexane	0.1	30 s	PA layer	53
10.	Zr porphyrin MOF	Dispersion (aqueous phase) vacuum filtration	0.005, 0.01, 0.02 and 0.03	Polyacrylonitrile -PAN	PIP	0.1	-	TMC / n-hexane		2 min	PA layer	54
11.	HKUST-1	Dispersion (aqueous phase and organic phase)	0.05, 0.1	Cellulose Nitrate (CN) and Cellulose Acetate (CA) CA/CN (1:3)	PIP	4	-	TMC / naphtha	0.24	-	PA layer	55
		In-situ growth		1, 6 Hexamethylenediamine (HDA): isopropyl alcohol (IPA) modified Polyimide - PI (P84)	PIP	1	2 min	TMC / n-hexane	0.1	30 s	Interlayer	56

while electrostatic repulsion occurs when interaction occurs between the membrane's surface charge interacts and the dye's charge[71]. The adsorption and/or rejection of dye molecules by TFN membranes are significantly influenced by their surface charge and MW. The charge on the dye controls the electrostatical interaction with the membrane surface, indicating whether it remains or is able to go through. In meantime, the MW controls the size of the dye molecule in relation to the membrane pores, which influences its capacity to pass through the membrane or filtered out. These elements work together to help us understand and maximize the separation efficiency of TFN membranes[72]. Table 4 presents a systematic tabulation for filtration setup and performance analysis of different MOF TFN membranes used in dye removal. All the abbreviations used throughout the article are given in the Supplementary Information.

Table 3 — Characterization of MOF and TFN membrane used in dye removal

S.No.	MOF type	MOF characterization										TFN Membrane characterization												Ref.
		SEM	TEM	XRD	STEM-HAADF	BET	FTIR	TGA	XPS	EDX	ICP	SEM	TEM	FTIR	XRD	XPS	STEM	EDS	EDX	AFM	MWCO	Pore size	HSP	Water contact angle	Zeta potential	
1.	UiO-66 and UiO-66-NH_2		✓	✓		✓		✓	✓	✓		✓	✓			✓				✓	✓			✓	✓	43
	UiO-66	✓		✓		✓		✓				✓	✓	✓	✓	✓							✓	✓		44
	UiO-66-NH_2, Ag@UiO-66-NH_2		✓	✓		✓					✓	✓						✓						✓		69
	UiO-66, UiO-66-$(NH_2)_2$ and UiO-66-$(NH_2)_2$ TMC	✓				✓	✓		✓			✓				✓				✓				✓	✓	70
2.	MOF-808	✓	✓		✓		✓	✓	✓		✓	✓			✓			✓		✓			✓	✓		43
3.	ZIF-8													✓		✓				✓	✓			✓		45
		✓		✓		✓		✓				✓	✓	✓	✓	✓							✓	✓		44
												✓			✓											42
				✓		✓						✓		✓	✓	✓				✓					✓	47
4.	MIL-101 (Cr)											✓			✓											42
			✓	✓								✓				✓	✓	✓		✓						49
5.	ZIF-93											✓			✓											42
												✓		✓	✓					✓				✓		50
				✓		✓		✓				✓			✓											51
		✓		✓		✓		✓				✓	✓	✓	✓	✓							✓	✓		44
6.	Fe MOF			✓			✓					✓		✓	✓									✓	✓	52
7.	Ag MOF	✓		✓			✓					✓		✓	✓	✓						✓		✓	✓	53
8.	Zr porphyrin MOF	✓	✓	✓			✓					✓							✓					✓	✓	54
9.	HKUST-1	✓		✓		✓	✓					✓		✓		✓				✓				✓		55
		✓		✓			✓					✓		✓		✓								✓	✓	56

Table 4 — Filtration setup, conditions and dye removal efficiency of different MOF-TFN membranes

S. No.	Membrane	MOF	MOF loading (wt.%)	Filtration setup	Operating Pressure	Effective membrane area	Solvent	Conc. (ppm)	Dye	Solute flux (LMH $Lm^{-2}h^{-1}$) (Highest)	Rejection % (Highest)	Ref.
1.	UiO-66@MoS_2 TFN	UiO-66,	0.01	Dead-end	20 bar	4.9 cm^2	Water	20	RB	8.29	99.6	43
									SY	12.03	98.4	
									AO	5.03	99.8	
	UiO-66-NH_2 @Mo_2 TFN	UiO-66-NH_2	0.01	Dead-end	20 bar	4.9 cm^2	Water	20	RB	6	99.6	
									SY	8.72	99.1	
									AO	4.99	99.7	
	MOF-808 @MoS_2 TFN	MOF-808	0.01	Dead-end	20 bar	4.9 cm^2	Water	20	RB	8.47	99.6	
									SY	10.33	99.3	
									AO	5.88	99.6	
2.	HKUST-1 TFN (organic)	HKUST-1	0.5	Dead-end	1 bar	0.2×10^{-2} m^2	Water	10	SY		89	55
									CR	28	96	
									AZ		90	
	HKUST-1 TFN (aqueous)	HKUST-1	0.5	Dead-end	1 bar	0.2×10^{-2} m^2	Water	10	SY		76	
									CR	123	78	
									AZ		75	

(*Contd*.)

Table 4 — Filtration setup, conditions and dye removal efficiency of different MOF-TFN membranes (*Contd*.)

S. No.	Membrane	MOF	MOF loading (wt.%)	Filtration setup	Operating Pressure	Effective membrane area	Solvent	Conc. (ppm)	Dye	Solute flux (LMH $Lm^{-2}h^{-1}$) (Highest)	Rejection % (Highest)	Ref.
3.	UiO-66-$(NH_2)_2$-TMC	UiO-66-$(NH_2)_2$	0.02 0.04 0.04	Cross-flow	0.4 MPa	23.75 cm^2	Water	100	AR CR MB	24.49 100.68 100.68	>95 98.82 91.29	70
4.	TFN	ZIF-8	0.5	Cross-flow	4 bar	7.0 cm^2	Water	100	RhB	5.5	99.9 %	47
5.	TFC HF	MIL-101(Cr) ZIF-8 ZIF-93	N25L10 (N is no. of fibers and L is length in cm)	Cross-flow	6 bar	334 cm^2	-	20	RB	1.25 ± 0.01	99.6 ± 0.6	42
6.	Chitosan Fe MOF	Fe MOF	1.5 0.5 0.5 1.5	Cross-flow	1–4 bar	0.0015 m^2	Water	25	EBT MB RhB CR	48.9 ±1.1 20.0 ± 0.6 19.0 ± 0.9 49.8± 0.8	99.1 ±0.1 89.9 ± 1 88.6 ± 1 99.2± 0	52
7.	PA/ZIF-93/SWCNT/P84	ZIF-93	-	Dead-end	10 bar	-	Water Methanol Water Methanol Water Methanol	20	RB SY AO 	57.6 ± 5.2 84.5 ± 5.9 57.6 ± 5.2 84.5 ± 5.9 57.6 ± 5.2 84.5 ± 5.9	99.9 ± 3.3 99.8 ± 4.1 99.7 ± 3.5 99.5 ± 3.8 99.6 ± 3.8 98.8 ± 3.5	50
				Cross-flow (6 h) 1 $L{\cdot}min^{-1}$	10 bar	-	Water		RB	50.9±3.3	99.9± 1.9	
8.	Ag-MOF TFN	Ag-MOF	0.01	Dead-end	2 bar	12.56 cm^2	-	10	RhB MO MB	11.1 ±0.2 9.9 ±0.4 9.0 ±0.4	99.3 ±0.4 95.4 ±0.4 85	53
9.	Ag@UiO-66-NH_2 TFN	UiO-66-NH_2	-	Cross-flow	0.1 MPa	7.54 $\times 10^{-4}$ m^2	Water	10	RhB	-	99.6	69
10.	TFN-3D	Zr-porphyrin MOF	0.01	Cross-flow	0.4 MPa	7.065 × 10^{-4} m^2	Water	500	MB RB5 CR RhB DR23	110.4	~ 100	54
11.	PA/ HKUST-1 bilayer	HKUST-1	-	-	5 bar	18.50 cm^2	Methanol	50	Pri AF BB BBG 250 RB	52.6 70.4 66.8 95.9 59.9	99.2 96.8 93.4 98.8 99.4	56
12.	ZIF-8 TFN	ZIF-8	-	Cross-flow	0.6 MPa	18.5 cm^2	Methanol	10	MB AF RB Mb	-	95.57 99.05 99.98 99.96	45
13.	PA/ZIF-93 bilayer	ZIF-93	-	-	8 bar	-	Water	15	AO	0.61	~ 93	51

(*Contd*.)

Table 4 — Filtration setup, conditions and dye removal efficiency of different MOF-TFN membranes (*Contd*.)

S. No.	Membrane	MOF	MOF loading (wt.%)	Filtration setup	Operating Pressure	Effective membrane area	Solvent	Conc. (ppm)	Dye	Solute flux (LMH $Lm^{-2}h^{-1}$) (Highest)	Rejection % (Highest)	Ref.
14.	TFN (post treatment with DMSO)	ZIF-8 ZIF-93 UiO-66	0.2	Dead-end	20 bar	12 cm^2	Methanol	20	SY	8.5 11± 0.6 11± 0.7	95.2 93.1 97.9	44
15.	LS-TFN	MIL-101(Cr)	0.2	Dead-end	20 bar	12 cm^2	Methanol	20	RB SY	9.5 ± 2.1 10.1 ± 0.5	>96%, >90%	49

Conclusion

The MOF and MOF-based TFN membranes have shown great potential in efficient dye separation as highlighted in this review. The limitations associated with TFC membranes, such as permeability-selectivity limitations and low chemical stability, have been overcome by using MOF as nanofiller, resulting in high-performance TFN membranes. The introduction of MOF onto the TFC membranes has shown many advantages like enhanced water flux, improved dye rejection, surface functionality, fouling resistance and tunable pore size. These TFN membranes achieved exceptional performance in dye separation by molecular sieving, electrostatic repulsion and adsorption. Furthermore, future research on MOF-based TFN membranes for dye removal should be directed towards the development of environmentally friendly and efficient membrane systems with water stable MOFs applicable for practical wastewater treatment. The stability of different MOFs in aqueous environments should be explored. Research should focus on green synthesis strategies with water-based solvents and eco-friendly linkers for the fabrication of MOFs to decrease the environmental footprint. Future research should work on optimizing interfacial polymerization to produce uniform MOF dispersion while avoiding nanofiller agglomeration, which is a significant obstacle for producing defect-free selective layers. Future studies should also focus on antifouling and self-cleaning TFN membranes by embedding photocatalytic or antimicrobial MOFs to sustain operational performance over an extended period of time under realistic conditions. Moreover, the evaluation of membrane performance using real industrial wastewater including complex combinations of colours and co-existing pollutants rather than model dye solutions alone is necessary for the assessment of practical application. Advanced computational tools, such as molecular simulations and machine learning, might possibly accelerate the rational design and optimization of membrane materials by anticipating structure–property connections and separation performance. Finally, to bridge the gap between laboratory-scale research and large-scale industrial implementation of MOF-based TFN membranes for sustainable dye wastewater treatment, studies on scalable fabrication techniques, standard performance evaluation protocols, and techno-economic assessments will be required. In summary, the MOF and MOF TFN membranes have shown great potential in wastewater treatment applications, especially dye separation, with further research and development, they can play an important role in mitigating global water-related issues. Target-specific and engineering development are crucial for bridging the gap between laboratory and industrial-scale practice.

Acknowledgments

The authors extend their appreciation to the National Institute of Technology, Raipur for their ample facility offerings and steadfast support.

Conflict of Interest

The authors declare that there are no conflicts of interest associated with this work.

Abbreviation

TFC – Thin film composite
TFN – Thin film nanocomposite
MOF (Metal Organic Framework)
HKUST-1 (Hong Kong University of Science and Technology-1)
ZIF-93 (Zeolitic Imidazolate Frameworks-93)
MIL-101 (Matérial Institut Lavoisier-101)
ZIF-8 (Zeolitic Imidazolate Frameworks-8)
UiO-66 (University of Oslo-66)
DMF – Dimethylformamide

DMSO-dimethyl sulfoxide
RO – Reverse osmosis
NF – Nanofiltration
MPD- m-phenylenediamine
PPD- P-phenylenediamine
TMC- Trimesoyl chloride
PIP- Piperazine
SDS- Sodium dodecyl sulfate
PA- Polyamide
IP – Interfacial polymerization
MW – Molecular weight
SWCNT- Single-walled carbon nanotube
HF – Hollow fibre
SEM-Scanning Electron Microscopy
TEM-Transmission Electron Microscopy
XRD-X-ray Diffraction
STEM-HAADF - Scanning Transmission Electron Microscopy High-Angle Annular Dark Field
BET- Brunauer Emmett Teller
FTIR-Fourier-Transform Infrared Spectroscopy
TGA-Thermogravimetric Analysis
XPS-X-ray Photoelectron Spectroscopy
STEM-Scanning Transmission Electron Microscopy
EDX-Energy-Dispersive X-ray Spectroscopy
ICP-Inductively Coupled Plasma
AFM- Atomic Force Microscopy
MWCO-Molecular Weight Cut-Off
HSP-Hansen solubility Parameters
RB-Rose Bengal
SY-Sunset Yellow
AO-Acridine Orange
AZ-Alphazurine
CR-Congo Red
MB-Methylene Blue
RhB-Rhodamine B
EBT-Eriochrome black t
MO-Methyl Orange
(RB-5) -Reactive Black 5
(DR-23) -Direct Red 23
BBG 250 - Brilliant Blue G 250
BB -Bromophenol Blue
Pri - Primuline
AF-Acid Fuchsin

References

1 Kolya H & Kang C W, Toxicity of metal oxides, dyes, and dissolved organic matter in water: Implications for the environment and human health, *Toxics*, 12 (2024) 111.

2 Periyasamy A P, Recent advances in the remediation of textile-dye-containing wastewater: Prioritizing human health and sustainable wastewater treatment, *Sustainability*, 16 (2024) 495.

3 Adane T, Adugna A T & Alemayehu E, Textile industry effluent treatment techniques, *J Chem*, 2021 (2021) 5314404.

4 Jahan N, Tahmid M, Shoronika A Z, Fariha A, Roy H, Pervez Md N, Cai Y, Naddeo V, Islam M S, A comprehensive review on the sustainable treatment of textile wastewater: Zero liquid discharge and resource recovery perspectives, *Sustainability*, 14 (2022) 15398.

5 Bhatia D, Sharma N R, Singh J & Kanwar R S, Biological methods for textile dye removal from wastewater: A review, *Crit Rev Environ Sci Technol*, 47 (2017) 1393263.

6 Chakraborty T K, Ghosh S, Islam M S, Nice M S, Islam K R, Netema B N, Rahman M S, Habib A, Zaman S, Ghosh G C, Hossain M R, Coubra K T, Adhikary K, Munna A, Haque M M, Bosu H & Halder M, Removal of hazardous textile dye from simulated wastewater by municipal organic solid waste charcoal using machine learning approaches: Kinetics, isotherm, and thermodynamics, *Heliyon*, 9 (2023) 18856.

7 Dutta S, Gupta B, Srivastava S K & Gupta A K, Recent advances on the removal of dyes from wastewater using various adsorbents: A critical review, *Mater Adv*, 2 (2021) 4497.

8 Khan S, Noor T, Iqbal N & Yaqoob L, Photocatalytic dye degradation from textile wastewater: A review, *ACS Omega*, 9 (2024) 21751.

9 Yagub M T, Sen T K, Afroze S & Ang H M, Dye and its removal from aqueous solution by adsorption: A review, *Adv Colloid Interf Sci*, 209 (2014) 172.

10 Dutta S, Adhikary S, Bhattacharya S, Roy D, Chatterjee S, Chakraborty A, Banerjee D, Ganguly A, Nanda S & Rajak P, Contamination of textile dyes in aquatic environment: Adverse impacts on aquatic ecosystem and human health, and its management using bioremediation, *J Environ Manag*, 353 (2024) 120103.

11 Ramamurthy K, Priya P S, Murugan R & Arockiaraj J, Hues of risk: investigating genotoxicity and environmental impacts of azo textile dyes, *Environ Sci Pollut Res*, 31 (2024) 33190.

12 Katheresan V, Kansedo J & Lau S Y, Efficiency of various recent wastewater dye removal methods: A review, *J Environ Chem Eng*, 6 (2018) 4676.

13 Carmen Z & Daniela S, Textile organic dyes-characteristics, polluting effects and separation/elimination procedures from industrial effluents-A critical overview, 56 (2012) 32373.

14 Kusumlata, Ambade B, Kumar A & Gautam S, Sustainable solutions: Reviewing the future of textile dye contaminant removal with emerging biological treatments, *Limnol Rev*, 24 *(*2024) 126.

15 Bal G & Thakur A, Distinct approaches of removal of dyes from wastewater: A review, *Mater Today Proc*, 50 (2022) 1575.

16 Valappil R S K, Ghasem N & Al-Marzouqi M, Current and future trends in polymer membrane-based gas separation technology: A comprehensive review, *J Ind Eng Chem*, 98 (2021) 103.

17 Agboola O, Fayomi O S I, Ayodeji A, Ayeni A O, Alagbe E E, Sanni S E, Okoro E E, Moropeng L, Sadiku R, Kupolati K W & Oni B A, A review on polymer nanocomposites and their effective applications in membranes and adsorbents for water treatment and gas separation, *Membranes*, 11 (2021) 139.

18 Xu G R, An Z H, Wang M, Xu K, Zhao H L & Liu Q, Polyamide layer modulation for PA-TFC membranes Optimization: Developments, Mechanisms, and implications, *Sep Purif Technol*, 311 (2023) 123200.

19 Zirehpour A, Rahimpour A & Ulbricht M. Nano-sized metal organic framework to improve the structural properties and desalination performance of thin film composite forward osmosis membrane, *J Memb Sci*, 531 (2017) 59.

20 Wang D, Su H, Han S, Tian M & Han L, The role of microporous metal–organic frameworks in thin-film nanocomposite membranes for nanofiltration, *Sep Purif Technol*, 333 (2024) 125859.

21 Kamali K, Mohammadi T & Zarghami S, Thin film composite nanofiltration membrane mediated by MOF interlayer with novel MOF templating technique for water treatment, *Ind Eng Chem Res*, 64 (2025) 16299.

22 Yu S, Li C, Zhao S, Chai M, Hou J & Lin R, Recent advances in the interfacial engineering of MOF-based mixed matrix membranes for gas separation, *Nanoscale*, 16 (2024) 7716.

23 Yang F, Du M, Yin K, Qiu Z, Zhao J, Liu C, Zhang G, Gao Y & Pang H, Applications of metal-organic frameworks in water treatment: A review, *Small*, 18 (2022) 2105715.

24 Zeggai F Z, Ait-Touchente Z, Bachari K & Elaissari A, Investigation of metal-organic frameworks (MOFs): synthesis, properties, and applications an in-depth review, *Chem Phys Impact*, 10 (2025) 100864.

25 Stock N & Biswas S, Synthesis of metal-organic frameworks (MOFs): Routes to various MOF topologies, morphologies, and composites, *Chem Rev*, 112 (2011) 933.

26 Raptopoulou C P, Metal-organic frameworks: Synthetic methods and potential applications, *Materials*, 14 (2021) 310.

27 Mahreni M & Ristianingsih Y, A review on Metal-Organic Framework (MOF): Synthesis and Solid Catalyst Applications, *Conf Ser Proc Eng Sci Ser*, 1 (2020) 638.

28 Udaya R R, Mathew T, Kumar H, Singhal A & Thomas L, Metal-organic frameworks: Recent advances in synthesis strategies and applications, *Inorg Chem Commun*, 162 (2024) 112223.

29 Derbe T, Sani T, Amare E & Girma T, Mini review on synthesis, characterization, and application of zeolite@MOF composite, *Adv Mater Sci Eng*, 2023 (2023) 8760967.

30 Głowniak S, Szczęśniak B, Choma J & Jaroniec M, Advances in microwave synthesis of nanoporous materials, *Adv Mater*, 33(2021) 2103477.

31 Dourandish Z, Tajik S, Beitollahi H, Jahani P M, Nejad F G, Sheikhshoaie I & Bartolomeo A D, A comprehensive review of metal-organic framework: Synthesis, characterization, and investigation of their application in electrochemical biosensors for biomedical analysis, *Sensors*, 22 (2022) 2238.

32 Phan P T, Hong J, Tran N & Le T H, The properties of microwave-assisted synthesis of metal–organic frameworks and their applications, *Nanomaterials*, 13 (2023) 352.

33 Gao Y, Wang F, Wang C C & Yi X H, Microwave-assisted production of metal-organic frameworks for water purification: A mini-review, *Surf Interf*, 44 (2024) 103724.

34 Lee Y R, Kim J & Ahn W S, Synthesis of metal-organic frameworks: A mini review, *Korean J Chem Eng*, 30 (2013) 1667.

35 Yusuf V F, Malek N I & Kailasa S K, Review on metal-organic framework classification, synthetic approaches, and influencing factors: Applications in energy, drug delivery, and wastewater treatment, *ACS Omega*, 7 (2022) 44507.

36 Lalawmpuia R, Lalhruaitluangi M & Tiwari D, Metal organic framework (MOF): Synthesis and fabrication for the application of electrochemical sensing, *Environ Eng Res*, 29 (2024) 230636.

37 Ren H & Wei T, Electrochemical synthesis methods of metal-organic frameworks and their environmental analysis applications: A review, *Chem Electro Chem*, 9 (2022) 196.

38 Wang Z & Wöll C, Fabrication of metal-organic framework thin films using programmed layer-by-layer assembly techniques,*Adv Mater Technol*, 4 (2019) 1800413.

39 Shekhah O., Layer-by-layer method for the synthesis and growth of surface mounted metal-organic frameworks (SURMOFs), *Materials*, 2 (2010) 1302.

40 Li D, Yadav A, Zhou H, Roy K, Thanasekaran P & Lee C, Advances and applications of metal-organic frameworks (MOFs) in emerging technologies: A comprehensive review, *Glob Chall*, 8 (2024) 2300244.

41 Brown A J, Brunelli N A, Eum K, Rashidi F, Johnson J R, Koros W J, Jones C W & Nair S, Interfacial microfluidic processing of metal-organic framework hollow fiber membranes, *Science*, 345 (2014) 72.

42 Esteras-Saz J, Paseta L, Echaide-Górriz C, Malankowska M, Luque-Alled J M, Zornoza B, Téllez C & Coronas J, Microfluidic preparation of thin film composite hollow fiber membrane modules for water nanofiltration: Up-scaling, reproducibility and MOF based layers, *J Taiwan Inst Chem Eng*, 150 (2023) 105063.

43 Colás-Sebastián J, Luque-Alled J M, Téllez C & Coronas J, Enhanced flux of nanofiltration membranes for low molecular weight solutes using Zr-MOF@MoS_2 nanohybrids as both interlayer and filler materials, *J Water Process Eng*, 78 (2025) 108642.

44 Paseta L, Navarro M, Coronas J & Téllez C, Greener processes in the preparation of thin film nanocomposite membranes with diverse metal-organic frameworks for organic solvent nanofiltration, *J Ind Eng Chem*, 77 (2019) 344.

45 Li P, Zhang M, Zhai Z, Wang M, Li P, Hou Y, Jason Q & Niu, Precise assembly of a zeolite imidazolate framework on polypropylene support for the fabrication of thin film nanocomposite reverse osmosis membrane, *J Memb Sci*, 612 (2020) 118412.

46 García-Palacín M, Martínez J I, Paseta L, Deacon A, Johnson T, Malankowska M, Tellez C & Coronas J, Sized-controlled ZIF-8 nanoparticle synthesis from recycled mother liquors: environmental impact assessment, *ACS Sustain Chem Eng*, 8 (2020) 2973.

47 Jia M M, Feng J H, Shao W, Chen Z, Yu J R, Sun J J, Wu Q Y, Li Y, Xue M & Chen X M, In-situ interfacial synthesis of metal-organic framework/polyamide thin-film nanocomposite membranes with elevated nanofiltration performances, *J Memb Sci*, 694 (2024) 122418.

48 Echaide-Górriz C, Aysa-Martínez Y, Navarro M, Téllez C & Coronas J, Polyamide-MIL-101(Cr) thin films synthesized on either the outer or inner surfaces of a polysulfone hollow fiber for water nanofiltration, *ACS Appl Mater Interf*, 13 (2021) 7773.

49 Navarro M, Benito J, Paseta L, Gascón I, Coronas J & Téllez C, Thin-film nanocomposite membrane with the minimum amount of mof by the langmuir-schaefer technique for nanofiltration, *ACS Appl Mater Interf*, 10 (2018) 1278.

50 Berned-Samatán V, Piantek M, Coronas J & Téllez C, Nanofiltration with polyamide thin film composite membrane with ZIF-93/SWCNT intermediate layers on polyimide support, *Sep Purif Technol*, 308 (2023) 308.

51 Echaide-Górriz C, Zapata J A, Etxeberría-Benavides M, Téllez C & Coronas J, Polyamide/MOF bilayered thin film composite hollow fiber membranes with tuned MOF thickness for water nanofiltration, *Sep Purif Technol*, 236 (2020) 116265.

52 Maraddi A, Halakarni M, Halanur M M & Nataraj S K, Fe-MOF induced biopolymer-based sustainable self-cleaning membranes for effective selective separation and wastewater treatment, *Sustain Mater Technol*, 35 (2023) 537.

53 Tan Z K, Gong J L, Fang S Y, Li J, Cao W C & Chen Z P, Outstanding anti-bacterial thin-film composite membrane prepared by incorporating silver-based metal-organic framework (Ag-MOF) for water treatment, *Appl Surf Sci*, 590 (2022) 153059.

54 Zhao P, Wang J, Han X, Liu J, Zhang Y & Van Der Bruggen B, Zr-porphyrin metal-organic framework-based photocatalytic self-cleaning membranes for efficient dye removal, *Ind Eng Chem Res*, 60 (2021) 1850.

55 Dubovenko R, Dmitrenko M, Mikulan A, Puzikova M, Dzhakashov I, Rakovskaya N, Kuzminova A, Mikhailovskaya O, Su R & Penkova A, Thin-film composite polyamide membranes modified with HKUST-1 for water treatment: Characterization and nanofiltration performance, *Polymers*, 17 (2025) 091137.

56 Chen K, Li P, Zhang H, Sun H, Yang X, Yao D, Pang X, Han X & Niu Q J, Organic solvent nanofiltration membrane with improved permeability by in-situ growth of metal-organic frameworks interlayer on the surface of polyimide substrate, *Sep Purif Technol*, 251 (2020) 117387.

57 Nambi K J, Venkatachalam K R, Ghosh O, Jhaveri K, Palakodeti A & Nair N, Review of thin film nanocomposite membranes and their applications in desalination, *Front Chem*, 10 (2022) 781372.

58 Farahbakhsh J, Vatanpour V, Khoshnam M & Zargar M, Recent advancements in the application of new monomers and membrane modification techniques for the fabrication of thin film composite membranes: A review, *React Funct Polym*, 166 (2021) 105015.

59 Lestari R A, Elma M, Syauqiah I, Roilbilad M & Rahma A, Modification of polyamide thin film-based membranes for water separation: A review, *J Chem Rev*, 7 (2025) 674.

60 Chong H Y, Muhammad S A H, Norazmi S N, Chang Z H & Teow Y H, A review on membrane fabrication: structure, properties and performance relationship, *J Appl Membr Sci Technol*, 29 (2025) 73.

61 Lau W J, Ismail A F, Misdan N & Kassim M A, A recent progress in thin film composite membrane: A review, *Desalination*, 287 (2012) 190.

62 Liu F, Wang L, Li D, Liu Q & Deng B, A review: The effect of the microporous support during interfacial polymerization on the morphology and performances of a thin film composite membrane for liquid purification, *RSC Adv*, 9 (2019) 35417.

63 Wei J, Liu X, Qiu C, Wang R & Tang C Y, Influence of monomer concentrations on the performance of polyamide-based thin film composite forward osmosis membranes, *J Memb Sci*, 381 (2011) 110.

64 Tayel A, Abdelaal A B, Esawi A M K & Ramadan A R, Thin-film nanocomposite (TFN) membranes for water treatment applications: Characterization and performance, *Membranes*, 13 (2023) 477.

65 Ismail A F, Padaki M, Hilal N, Matsuura T & Lau W J, Thin film composite membrane-recent development and future potential, *Desalination*, 356 (2015) 140.

66 Zhang L, He Y & Fu Y, Recent innovations in in situ strategies to prepare metal-organic framework-based mixed matrix membranes, *Chem Commun*, 61 (2025) 2878.

67 Zhao Y Y, Liu Y L, Wang X M, Huang X & Xie Y F, Impacts of metal-organic frameworks on structure and performance of polyamide thin-film nanocomposite membranes, *ACS Appl Mater Interf*, 11 (2019) 13724.

68 Jia Y, Huo X, Gao L, Shao W & Chang N, Controllable design of polyamide composite membrane separation layer structures via metal-organic frameworks: A review, *Membranes*, 14 (2024) 201.

69 Bai X, Ma W, Liu P, Sun Q, Zhang K, Li A, Pan J & Lyu Z, Catalytic TFN membranes containing MOF loaded Ag NPs prepared by interfacial polymerization, *Micropor Mesopor Mater*, 335 (2022) 111811.

70 Huo X, Miao Y, Guo Z, Shi Z, Jia Y, Wang H & Chang N. Construction of low-resistance nano-transport channels with UiO-66-$(NH_2)_2$ “transmembrane” in polyamide layer structure for efficient nanofiltration, *Chem Eng J*, 497 (2024) 154488.

71 Liu Y, Zhu J, Chi M S, Eygen G V, Guan K & Matsuyama H, Comprehensive review of nanofiltration membranes for efficient resource recovery from textile wastewater, *Chem Eng J*, 506 (2025) 160132.

72 Maziya K, Kotze I, Richards HL. Enhancing dye rejection and antifouling resistance of thin film nanocomposite nanofiltration membranes by the incorporation of glutamic acid functionalized graphene oxide. *Front. Membr. Sci. Technol*, 4 (2025) 1571459.